ACTA TECHNICA CORVINIENSIS – Bulletin of Engineering
Tome V (Year 2012). FASCICULE 4 [October–December]. ISSN 2067-3809

[1.] Robert POSPICHAL, [2.] Gerhard LIEDL

SIMULATION OF THE RESULTING INTENSITY DISTRIBUTION BY MULTI-BEAM INTERFERENCE OF AN ULTRA-SHORT PULSE LASER

[1-2.] VIENNA UNIVERSITY OF TECHNOLOGY, INSTITUTE FOR PRODUCTION ENGINEERING & LASER TECHNOLOGY, GUSSHAUSSTRAßE 30, VIENNA, AUSTRIA

ABSTRACT: *During the last years, the self-cleaning surface structures of lotus flowers have been reproduced in numerous ways on textiles or paints and other surfaces to reduce sensitivity against pollution which, in turn, allows a reduction of water- and detergent consumption. Unfortunately, some of these techniques suffer from wear or are potentially biohazardous due to the small particle size. We present a method to produce nanostructures on surfaces by multi-beam interference of ultra-short laser pulses. Intensity distributions of various configurations have been simulated and show the feasibility of the suggested process.*
KEYWORDS: *lotus-effect, multi-beam interference, nano-structures, ultra-short pulse laser*

LOTUS-EFFECT

Lotus-effect is the self-cleaning ability of natural surfaces. It is named by Barthlott und Neinhuis [1] after the Lotus-plant, which shows selfsame characteristics. Nearly every ecosystem contains examples of this lotus-effect. Neinhuis and Barthlott did a very complete listing of the natural occurrences [1, 2].

The effect is based on two principles [3]:

Examples in nature show a hydrophobic surface, the so called cuticula, which consists in most cases of wax. This layer increases the interface tension between the leaf and the water droplet. As a consequence, the contact angle between surface and water droplet increases, too. It has been shown that it is possible that such wax layers may erode during plant growth, leaving plant surfaces almost smooth and without water-repellent properties [1].

The other main effect is based on the two-part surface structure:

Burlings (papillae) are placed on the cuticula. The burlings extend to a height up to 5 µm or 10 µm and placed at a distance between 10 µm and 15 µm next to each other. These papillae exhibit finer structures on their surfaces, where the actual nano-structure is superimposed by means of wax crystals. Usually, these crystals show diameters in the order of 100 nm [1].

Several studies have proved that a correlation between the existence of a two-part surface structure and the super-hydrophobic behavior exists. On the other hand, it has been shown that examples in nature exist, which exhibit one-part surface structures in the nanometer range with excellent super-hydrophobic behavior [4, 5].

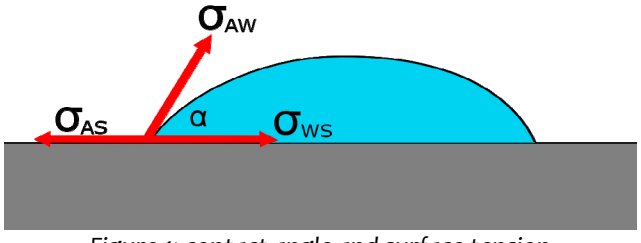

Figure 1: contact angle and surface tension

In any case, the contact area between water droplet and surface is minimized as well as adhesive forces. As a consequence, water droplets on the surface take a more or less spherical from. The contact angle between droplet and surface is used to characterize the hydrophobicity of surface structures.

The relation between surface tension and contact angle is characterized by the Young-Equation [6] (cf. Figure 1):

$$\cos(\alpha) = \frac{\sigma_{AS} - \sigma_{WS}}{\sigma_{AW}} \qquad (1)$$

This equation needs to be extended by the factor r for rough surfaces.r is the ratio between the real (rough) surface area and the area projected from the drop.

$$\cos(\alpha) = r \cdot \frac{\sigma_{AS} - \sigma_{WS}}{\sigma_{AW}} \qquad (2)$$

According to Onda [7], this equation loses its validity for fractal surfaces due to the fact that the right side of the equation increases much faster than one for larger values of r.

The contact angle has to be deduced form the effective surface tension between the fluid and the fractal surface, retrospectively between air and the fractal surface.

$$\cos(\alpha) = \frac{\alpha_{f13} - \alpha_{f12}}{\alpha_{23}} \qquad (3)$$

Onda also showed approximation formulas for the effective surface tension of fractal surfaces, which have been experimental verified. As described by Öner et al. [8], the wettability of surfaces is influenced by contact angle hysteresis, too. The difference between advancing and receding contact angles is important for hydrophobicity, since static contact angle measurements are not able to describe hydrophobic behaviour of surfaces in detail.

ENVIRONMENTAL IMPACT

It is clear that hydrophobic surfaces where pollutants can be removed easily or don't adhere at all have the potential to reduce usage of detergents dramatically.

On the other hand, production processes of hydrophobic surfaces will influence the environment, too.

The expected impact can be divided in two main parts: First at all, usage of materials which exhibit a lotus-effect will definitely influence the environment. Additionally, production processes with its unknown threats in environmental contamination have to be evaluated thoroughly. The process proposal presented here has a chance to influence both.

ENVIRONMENTAL IMPACT OF THE LOTUS EFFECT

The self-cleaning ability of surfaces will of course result in a reduced number of cleaning processes. The lotus-effect itself doesn't depend on any detergents. Therefore, water consumption as well as detergent consumption can be decreased substantially. Furthermore, in the case of outdoor applications where surfaces will be cleaned by rain water it is supposable that cleaning processes can be skipped completely.

The first stage of the presented project aims to produce plastic films with this self-cleaning ability. In further stages it is also planned to adopt the process to textile structures or even fibers. It is intended that the required structures should be produced by means of an ultra-short laser system.

In principle, the structuring off almost any material should be possible. Prior to that, a thorough understanding of the impact of different features and their shape and size is required. Additionally, an adequate laser source in terms sufficient pulse energy and duration and frequency is needed.

ENVIRONMENTAL IMPACT OF THE PROCESS

The conventional way of a hydrophobic finishing - for example for textiles - is a treatment with hydrophobic particles like fluorocarbons or silicon oils [9]. Such processes suffer from some disadvantages:

- *wash resistance of the finish is very limited or can just be guaranteed with large expenses [9]*
- *used chemicals are critical under an ecological as well as under an biological point of view [10]*
- *need of an own process, in case of textiles after the fiber production or after the textile assembly*

Therefore some environmental issues can be avoided if the lotus-effect is used instead of conventional chemicals. Most existing lotus-effect applications rely on a coating of the textile with a finish which contains the nano-particles.

Although no chemicals like fluorocarbons or silicon oils are needed any more, the nano-coating itself is also not harmless: Especially handling of the dry coating can be hazardous.

The danger originates from the particles itself: Due to the small particle size in the nanometer range, the particles are able to penetrate the respiratory system up to the lungs. This is on one hand dangerous cause some particles cannot be removed from the lungs and can therefore cause an immunoreaction. One the other hand, if particles are able to reach the blood circuit, they can evoke systematic damages in other organs [11].

Till now, biological threats which originating from a large scale usage of nanoparticles is not completely understood and especially long term effects cannot be judged. Additionally, nanoparticles can accumulate in the environment with almost unknown implications in the future.

In fact, the evaluation of the environmental impacts of nanoparticles is subject of numerous recent studies (e.g. [12,13, 11]).

The process described here offers the possibility for the production of hydrophobic surfaces without the need for dangerous chemicals and without the need for manipulation of potentially dangerous nanoparticles. The nano-scaled structure will be produced directly onto the surface of the sample and emission of nanoparticles occurs during the use of the product over long periods on low concentrations is avoided.

Moreover, it is expected that the process can be integrated into existing production lines easily. As a result, pollution of the environment is minimized as well as energy consumption of the process. In addition to advantages mentioned already, economic feasibility will be increased, too.

PROJECTED EXPERIMENTS

As already mentioned, an ultra-short pulse laser system will be used for experiments. The laser beam will be divided into several independent beams and interference between different beams will be used to produce the desired structures. The experimental set-up is described below.

The periodic structures for the lotus-effect will be fabricated by the ablation of material caused by interference of laser radiation. Therefore the laser beam will be divided by optical elements into at least two partial beams which will be recombined at the surface of the material.

From basic electromagnetic theory it is known that the total field strength of a combination of different electromagnetic fields is the sum of single field strengths. There sulting superposition of the field strengths of partial beams and since the intensitv is proportional to the square of the field strength, $I \propto E^2$, the intensity includes interference terms:

$$E = \sum E_{o,i} \cdot e^{-i(\vec{k}_i \cdot \vec{r} - \omega \cdot t + \phi_i)} \qquad (4)$$

The resulting field strength and therefore the resulting intensity distribution depend on the wave vectors. Therefore the easiest way to manipulate the resulting structures is to change the angle between partial beams. Further manipulation can be achieved by change of the phase relations or the polarization of the partial beams [14].

Beam separation into two or more partial beams can be done by optical elements like mirrors or grids. Beam guidance is done by mirrors; phase relation of the partial beams can be done with beam delay slides. Figure 2 and Figure 3show an example of a three-beam interference with the resulting intensity.

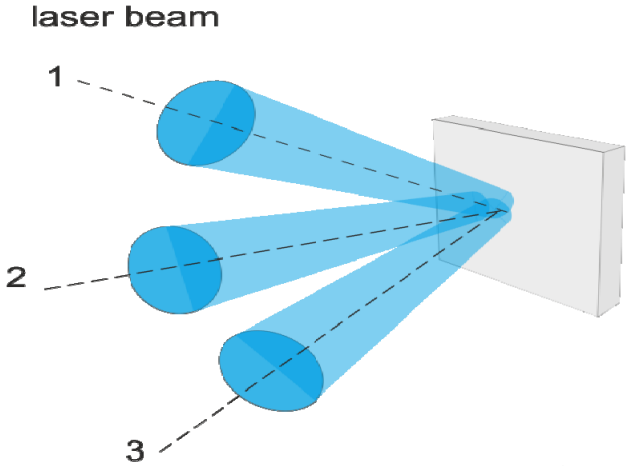

Figure 2: interfering beams under an angle of 120°

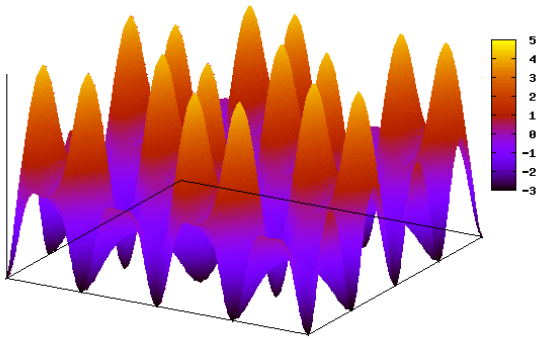

Figure 3: related intensity distribution

TWO-BEAM INTERFERENCE

First experiments will be done with a two-beam interference set-up. These experiments will help to identify the main parameters of the optical system and the laser system used for experiments. They will also help to find suitable methods for the evaluation of the produced structures.

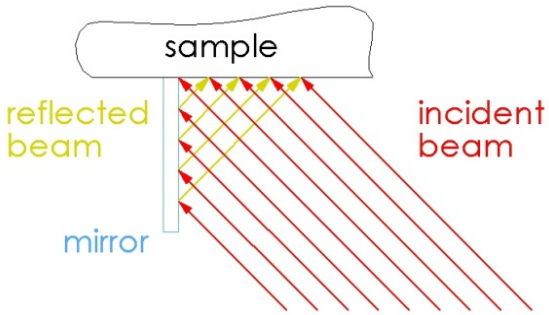

Figure 4: setup of Lloyds mirror

The easiest way of a two-beam interference is Lloyds mirror [14, 15], where a part of a beam interferes with its own reflection. Figure 4 shows the principle set-up. In general, every two beam interference results in a line shaped pattern. The production of grid shaped patterns can be achieved by two exposures, with a rotation of the sample in between.

A simulation of resulting interference pattern can be found in the simulation section.

MULTI-BEAM INTERFERENCE

There are innumerable ways to establish multi-beam interference e.g. with the use of grids, mirrors and beam delay slides in order to change angle and phase relation of partial beams [16], or by the use of a prism, where the incident beam will be divided into four partial beams which interfere at the sample surface, according to Wu et al. [17, 18].

Independent of the solutions used, the diameter of the partial beams has to be as large as possible to provide a huge treatment area. It has been shown by Fucetola et al. and Byun that processing of areas in the range of some mm² up to cm² [19,15] is possible.

The model presented in this paper is based on the so called diffractive variable delay generator (DVDG), presented by Klein-Wiele and Simon [14]. It consists mainly of two diffractive beam splitters followed by an aperture.

Two gratings, which are placed perpendicular to each other act as beam splitter. When the distance between them is adjustable, it is also possible to manipulate the phase relation between the two beam pairs. The angle between the partial beams results of the diffractive elements and the aperture.

The simulation section takes a more detailed view on this solution.

ULTRA-SHORT PULSE LASER

The experiments will be done with a laser with pulse duration in the sub picosecond range and a pulse frequency up to one MHz. Its fundamental wavelength is 1064 nm. SHG and respectively THG modules offer the possibility of emission of the second or third harmonic wavelength, what results in minimized interference pattern sizes. The raw beam diameter is about 1 mm with a beam divergence of 2.5 mrad.

SIMULATION

This section shows the expected interference pattern of the Lloyds mirror setup and the diffractive variable delay generator. The simulationswere done with the open source software Scilab, Version 5.3.3.

Both models include the parameters of the previously mentioned laser. Especially the wavelengths of 1064 nm, respectively 532 nm and 354.7 nm have been simulated.

LLOYDS MIRROR

The angle between sample and beam propagation direction has been defined with 45° in one simulation and 60° in the other. As the model is symmetric, the angle between mirror and beam propagation direction is the same.

A larger angle decreases the distance between the characteristic lines, a smaller increases it and also results in a lower intensity, as the exposed area increases.

The model consists mainly of two beams which propagate in the x-y layer at an angle of 90°, respectively 120°.The resulting intensity distribution has been calculated as the square of the sum of the electrical field $\vec{E}$.

$$E = E_1 \cdot e^{-i\cdot\vec{k}_1\cdot\vec{r}} + E_2 \cdot e^{-i\cdot\vec{k}_2\cdot\vec{r}} \quad (5)$$

$$I \propto E1^2 + E1^2 + 2E1E2\cos[(k1 - k2)r] \quad (6)$$

Amplitudes E_1 and E_2 were set constant to 1. The position vector goes from 0 to 5 µm in x- and y-direction; z-direction was set to 0. The considered wavelengths are inserted into the calculation through

the wave vector k, as its absolute value was set to $\frac{2\pi}{\lambda}$.

Figure 5 to 7 show the resulting intensity distribution with the first, second and third harmonic wavelength and an angle of 90° between incident and reflected beam:

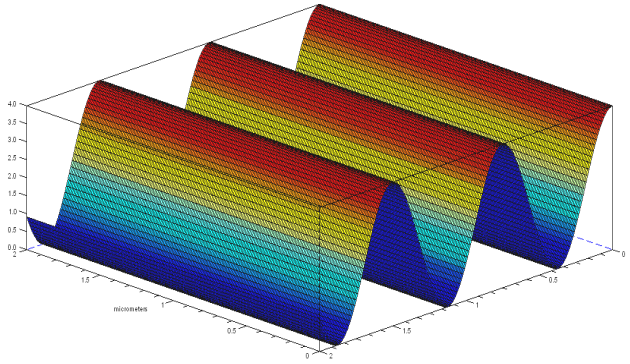

Figure 5: 90°, λ=1064 nm

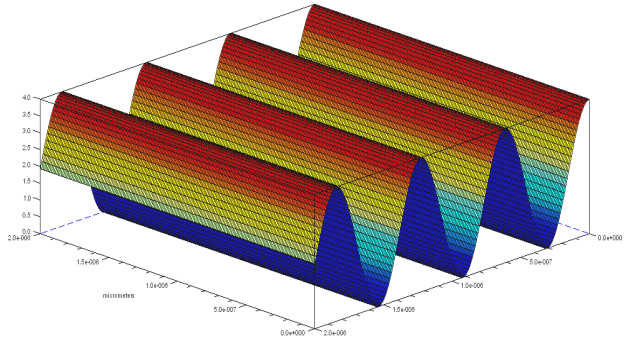

Figure 6: 90°, λ=532 nm

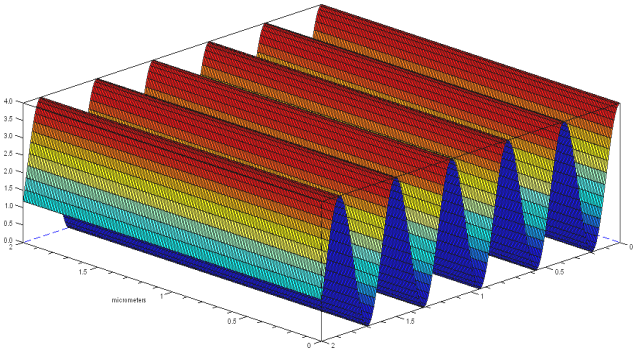

Figure 7: 90°, λ=354.7 nm

Figure 8 to 10 show selfsame with an angle of 120° between the partial beams.

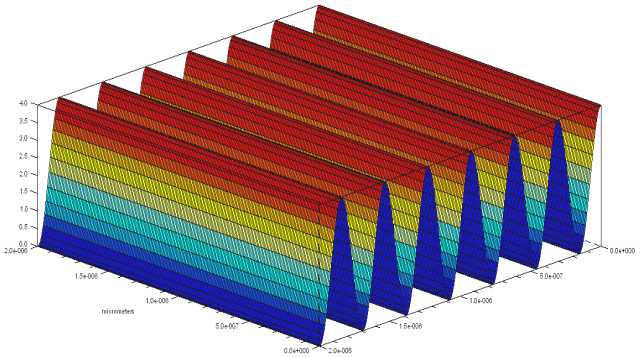

Figure 8: 120°, λ=1064 nm

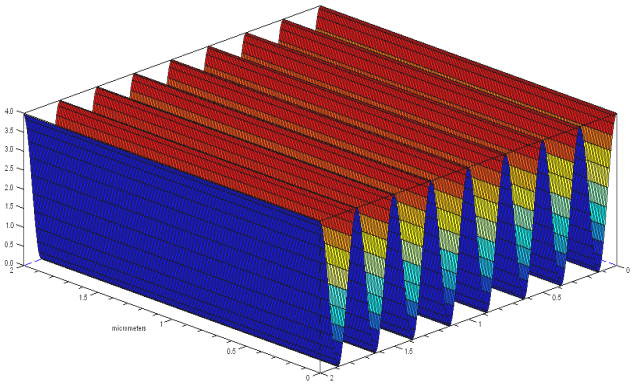

Figure 9: 120°, λ=532 nm

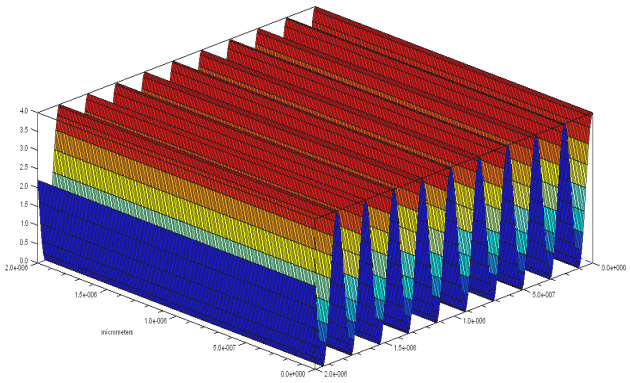

Figure 10: 120°, λ=352.7 nm

DIFFRACTIVE VARIABLE DELAY GENERATOR

The second model shows the possibilities of the diffractive variable delay generator.

At the beginning, the simplest experimental set-up has been simulated: two perpendicular pairs of beams without phase shift. First simulation has been done with an angle of 90° between the partial beams of each pair, the second simulation with an angle of 120°. Both configurations have been simulated with the first three harmonic wavelengths. Resulting intensity distribution includes between all four involved beams.

$$E = E_1 \cdot e^{-i\cdot\vec{k}_1\cdot\vec{r}} + E_2 \cdot e^{-i\cdot\vec{k}_2\cdot\vec{r}} + E_3 \cdot e^{-i\cdot\vec{k}_3\cdot\vec{r}} + E_4 \cdot e^{-i\cdot\vec{k}_4\cdot\vec{r}} \quad (7)$$

$$I \propto E^2 \quad (8)$$

Figures 11 to 13 show the resulting intensity distribution with an angle of 90° between the partial beams with the first three harmonic wavelengths:

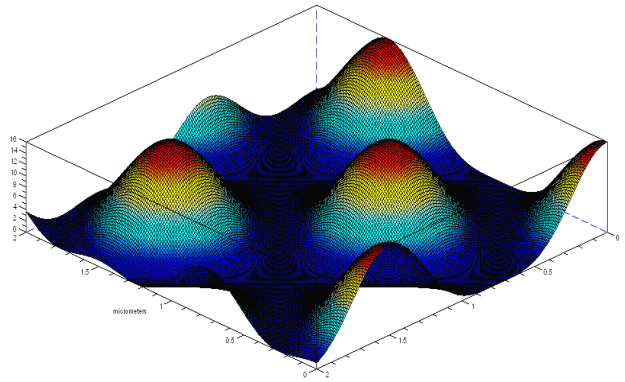

Figure 11: 90°, λ=1064 nm

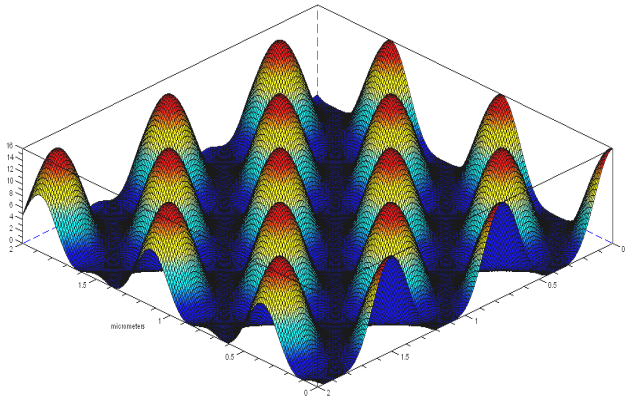

Figure 12: 90°, λ=532 nm

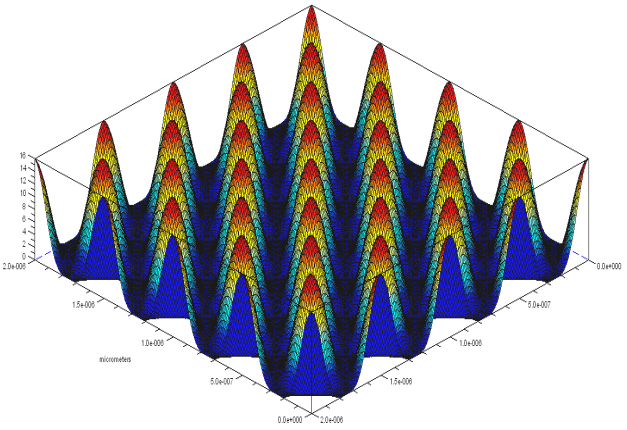

Figure 13: 90°, λ=354.7 nm

Figures 14 to 16 show simulation results with an angle of 120° between partial beams:

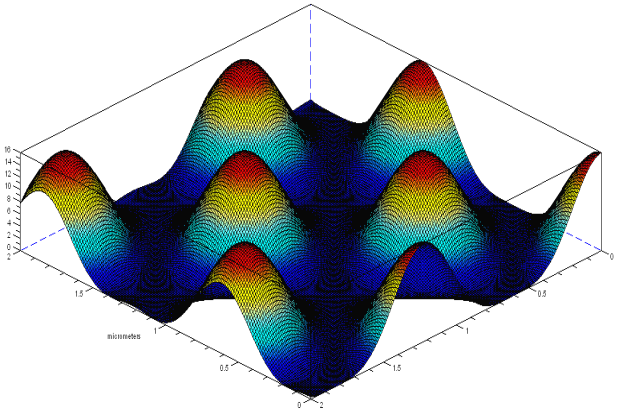

Figure 14: 120°, λ=1064 nm

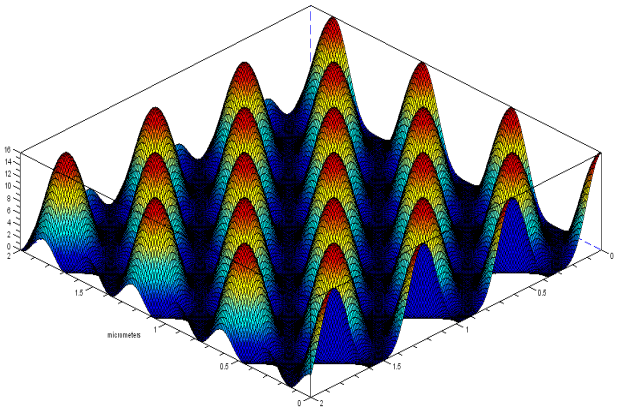

Figure 15: 120°, λ=532 nm

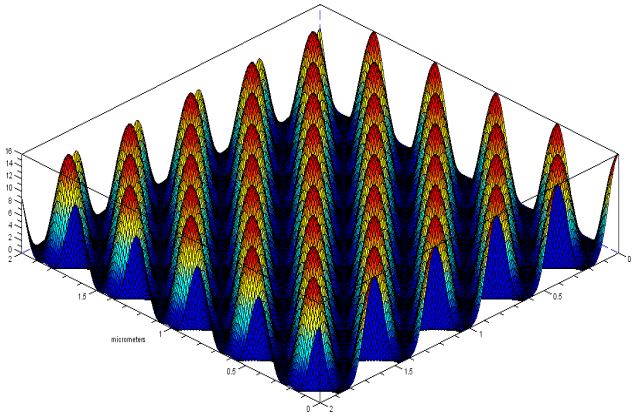

Figure 16: 120°, λ=354.7 nm

DISCUSSION AND OUTLOOK

First simulations show the feasibility of the fabrication of nanostructures in order to create a lotus-effect by multi-beam interference of ultra-short laser pulses.

As the simulation results with Lloyds mirror indicate, it seems possible to produce line-like structures with a width of about 100 nm, depending on wavelength and interference angle. A rotation of the sample after the exposure and a subsequent exposure should induce a grid shaped structure with a mesh size of about 100 nm x 100 nm. The model has to be extended to demonstrate this.

Simulation results achieved based on the model of the diffractive variable delay generator indicates that the fabrication of a grid with a mesh size of 200 nm x 200 nm in one step is possible. As a next step, the model will be extended by a phase shift between the two beam pairs, as Klein-Wiele and Simon [14] have shown a strong dependency of the pattern on the phase relations.

The model can also easily be extended by additional partial beams, which results in different features of the pattern.

Further simulations are necessary to estimate possible structures and their consequences on the wetting behaviour of samples. Additionally, the model has to be extended by material properties and absolute values of the optical intensity to clarify the dimensions of the resulting structures. Optical elements also have to be included to estimate the size of exposed area. Till now, polarization states as well as intensity distributions of real laser beams are not considered in simualtions presented here. Additional work has to be done to include all mentioned features. Nevertheless, results indicate a promising possibility for the production of nano-sized structures.

As next step, experimental verification of simulation results is of utmost importance. Based on these first experiments, a rough calculation of expected costs and energy consumption has to be done to estimate ecological as well as economic benefit.

REFERENCES

[1.] C.a.B.W. Neinhuis, Annals of Botany, 667 (1997).
[2.] T. Wagner, C. Neinhuis, W. Barthlott, ActaZoologica**77**, 213 (1996).
[3.] K.E. Jopp, Nanotechnologie - Aufbruch ins Reich der Zwerge, Gabler, Wiesbaden 2006.

[4.] E. Martines, K. Seunarine, H. Morgan, N. Gadegaard, C.D.W. Wilkinson, M.O. Riehle, Nano Lett**5**, 2097 (2005).
[5.] L. Feng, S. Li, H. Li, J. Zhai, Y. Song, L. Jiang, D. Zhu, Angew. Chem. Int. Ed**41**, 1221 (2002).
[6.] H. Wiese, Berichte der Bunsengesellschaft für physikalische Chemie**95**, 758 (1991).
[7.] T. Onda, S. Shibuichi, N. Satoh, K. Tsujii, Langmuir**12**, 2125 (1996).
[8.] D. Öner, T.J. McCarthy, Langmuir**16**, 7777 (2000).
[9.] H.-K. Rouette, Handbuch Textilveredlung, Dt. Fachverl, Frankfurt am Main 2006.
[10.] T. Platzek, Bundesgesundhbl**40**, 238 (1997).
[11.] J.M. Wörle-Knirsch, H.F. Krug, Nano Lett, 101 (2007).
[12.] N.R.C. Committee to Review the National Nanotechnology Initiative, A matter of size: Triennial review of the National Nanotechnology Initiative, National Academies Press, Washington, D.C 2006.
[13.] K. Klien, The genotoxic effects of FeCoB nanoparticles on human fibroblasts assessed by comet assay, Wien 2010.
[14.] J.-H. Klein-Wiele, P. Simon, Applied Physics Letters**83**, 4707 (2003).
[15.] I. Byun, J. Kim, J. Micromech. Microeng**20**, 55024 (2010).
[16.] M.-J. Mannini, TisserandStéphane, PengChangsi, S.M. Olaizola, DELILA Report: Development of Lithography Technology for Nanoscale Structuring of Materials Using Laser Beam Interference. Komplett 2006.
[17.] L. Wu, ZhongYongchun, Chan Che Ting, Wong Kam Sing, Wang, Guo Ping, Appl. Phys. Lett**86**, 2411021 (2005).
[18.] M. Lei, B.a.R.A.R. Yao, Optics Express**14**, 5803 (2006).
[19.] C.P. Fucetola, H. Korre, K.K. Berggren, J. Vac. Sci. Technol. B**27**, 2958 (2009).

ISSN: 2067-3809 [CD-Rom, online]